Chiang Mai Dental Journal

Original Article

In vitro Caries Inhibition in Enamel Adjacent to Ion-releasing Resin Composite

Sorrawis Kuphasuk[1], Sitthikorn Kunawarote[2]
[1]Private Practice, Thailand
[2]Department of Restorative Dentistry and Periodontology, Faculty of Dentistry, Chiang Mai University, Thailand

Received: January 3, 2022 • Revised: March 8, 2022 • Accepted: May 17, 2022

Corresponding Author: ***Assistant Professor Dr. Sitthikorn Kunawarote,*** *Department of Restorative Dentistry and Periodontology, Faculty of Dentistry, Chiang Mai University, Chiang Mai 50200, Thailand. (E-mail:* ***sitthikorn.k@cmu.ac.th****)*

Abstract

Objectives: To evaluate the nanohardness, mineral loss and lesion depth of the enamel adjacent to different restorative materials in conjugation with artificial caries induction.

Methods: Thirty-six human premolars with a prepared cylindrical cavity of 2 mm in diameter and depth. The specimens were randomly divided into 6 groups according to the restorative materials: Fuji IX GP®(GI), Cention N(CN) and Clearfil™ AP-X ES-2(RC) and adhesive systems: Clearfil™ SE bond X(CSE) and Adper™ Scotchbond™ multi-purpose (SBMP). Group 1; GI, Group 2; CN, Group 3; CN+CSE, Group 4; CN+SBMP, Group 5; RC+CSE and Group 6; RC+SBMP. All restored specimens were subjected to 14 days artificial caries induction then sectioned to two cross-sectional specimens (n=12). Nanohardness was evaluated at the depths of 10, 60, 110 and 160 μm from the enamel surface. Mineral loss and lesion depth of the enamel was evaluated at 10, 260, 510 and 760 μm from the tooth-restoration interface. Nanohardness data were analyzed using Wilcoxon-signed rank and Kruskal-Wallis test (p<0.05). Mineral loss and lesion depth data were analyzed using one-way ANOVA and Dunnett T3 (p<0.05).

Results: At the depth of 10 and 60 μm, the dissolution of enamel surface was observed for RC groups. At the depth of 10 μm, the nanohardness between the groups of GI and CN without adhesive showed no significant difference. At the distance of 10 μm from the tooth-restoration interface, the mineral loss and lesion depth of GI group showed no significant difference compared to those of the CN group.

Conclusions: Use of ion-releasing resin composite without adhesive exhibited a caries inhibition effect which was comparable to that of glass ionomer material.

Keywords: caries inhibition, ion-releasing resin composite, lesion dept, nanohardness, mineral loss

Introduction

Amalgam is a conventional material that has been widely used for restoring the posterior teeth. However, after the Minamata Agreement to phase down amalgam, many alternative materials were competitively developed.(1) The development of resin composites and adhesive systems has had a huge impact on restoring anterior and posterior teeth. These materials perform naturally esthetic properties and encourage conserving essential tooth structure.(2) However, resin composite materials are harden by means of polymerization reactions, therefore improper restorative procedures can cause undesirable polymerization shrinkage.(3) As a result of polymerization shrinkage, the complications such as cuspal deflection, post-operative hypersensitivity, and marginal leakage have occurred. Moreover, the resin composite marginal leakage is the fundamental cause of the secondary caries at the tooth-restoration interface.(4)

Secondary caries increases the failure rate of the restoration and can commonly be detected when a cavity was restored using amalgam or resin composite materials.[5] However, secondary caries is rarely observed at the enamel margin of a glass ionomer restored cavity.[6] These materials have ion-releasing properties, mainly fluoride ions that have the potential to inhibit caries formation on the tooth structure adjacent to the restoration.[6] Therefore, ion-releasing properties have been added to resin composite materials; these materials are classified as the ion-releasing resin composite.[7]

A new amalgam alternative material, Cention N (Ivoclar, Liechtenstein), has been introduced in the subgroup of the resin composite material called "alkasite". An alkasite is an ion-releasing resin composite material consisting of alkaline fillers. Once placed in acidic conditions, these fillers exhibited a higher capability in releasing calcium and fluoride ions.[8] These ions prevent demineralization and enhance remineralization of tooth structures adjacent to the restoration. Moreover, hydroxyl ions released from the fillers have the potential to neutralize the acidic circumstance. In addition, as this material polymerizes with a dual-cure reaction, it has an ability to be used as a full bulk replacement and can be used with or without adhesive application.[8] An *in vitro* study reported that when immersed in artificial saliva, the material formed an apatite layer on its surface. Consequently, the bioactive properties of this material could explain the low incidence of clinical secondary caries found.[9]

Previous studies have investigated the behaviors of the enamel at the restoration margin under the artificial caries induction. Serra and Cury reported that the adjacent enamel of the glass ionomer restoration exhibited the ability to maintain its mineral density and microhardness.[10] Micro-computed tomography (micro-CT) has been acknowledged as an accurate quantitative mineral density investigating tool for human hard tissues. Moreover, utilization of micro-CT incorporates an image processing program that requires a simple and non-destructive specimen preparation.[11] The mechanical properties of enamel reflect its composition and mineralization or mineral status. Nanoindentation is a wildly employed measurement for local hardness, modulus, toughness and friction properties of dental hard tissue and materials.[12,13]

In order to understand the influence of the recently marketed ion-releasing resin composite on secondary caries inhibition, the integrated mineral profile and mechanical properties of the adjacent enamel must be evaluated. The purpose of this study was to evaluate the caries inhibition behaviors of the contiguous enamel when the tooth cavity was restored using ion-releasing resin composite with and without adhesive system in conjugation with an artificial caries induction on the nanohardness, mineral loss, and lesion depth. The null hypothesis tested was that different restorative materials would not affect the caries inhibition property on the contiguous enamel.

Materials and Methods

This study was approved by the Human Experimentation Committee, Faculty of Dentistry, Chiang Mai University, Thailand (NO.16/2020).

Materials

In this laboratory study, three different types of restorative materials with a shade of A2 were used: GI (Fuji IX GP® Extra, GC Corp., Japan), a hand mixed conventional glass ionomer; CN (Cention N, Ivoclar , Liechtenstein), a hand mixed ion-releasing resin composite; and RC (Clearfil™ AP-X ES-2, Kuraray Noritake Dental Inc., Japan), a conventional resin composite along with two different adhesive systems: CSE (Clearfil™ SE bond X, Kuraray Noritake Dental Inc., Japan), a two-step self-etch adhesive system; and SBMP (Adper™ Scotchbond™ multi-purpose, 3M ESPE, USA), a three-step etch and rinse adhesive system. The details of each restorative material and adhesive system are given in Table 1.

Specimen preparation

The procedure of specimen preparation is summarized and illustrated in Figure 1. Thirty-six human premolars without carious lesion or other defects were used in this study. They were immersed in 0.1% thymol solution and used within 3 months of storage. All teeth were first sectioned by a precision diamond saw (IsoMet™ 1000, Buehler, USA) at the cemento-enamel junction then through the mesio-distal direction of the crowns. After that, the individual buccal section with the enamel surface faced up was embedded in a self-curing acrylic resin. The buccal enamel surface was ground with silicon carbide paper of 600 grit to obtain a flat surface. Consequently, a

Table 1: The details of the restorative materials and adhesive systems

Material	Type	Manufacturer	Lot number	Composition	Instructions
Fuji IX GP® Extra (shade A2)	Convention glass ionomer cement	GC Corp.; Japan	1812041	**Powder:** alumino-fluoro-silicate glass and polyacrylic acid powder. **Liquid:** distilled water, polyacrylic acid and polybasic carboxylic acid.	- Apply dentin conditioner to the cavity surface for 20 seconds, rinse thoroughly with water then gently air dry. - Mix the material with a power to liquid ratio of 1:1 (mixing time; 30 seconds and setting time; 2.20 minutes.) - Coat the material with resin coating and light-cured for 10 seconds.
Cention N (shade A2)	Ion-releasing resin composite (alkasite)	Ivoclar; Liechtenstein	Y29959	**Powder:** calcium fluorosilicate glass, barium aluminium silicate glass, ytterbium trifluoride, calcium barium aluminium fluoro-silicate glass, isofiller, initiator and pigment **Liquid:** dimethacrylate, initiators, additive and stabiliser **Filler loading:** 78.4 wt%, 57.6 vol%	- Mix the material with a power to liquid ratio of 1:1 (mixing time; 40-60 seconds and setting time; 5 minutes) - Light-cured for 20 seconds.
Clearfil™ AP-X ES-2 (shade A2)	Conventional resin composite	Kuraray Noritake Dental Inc.; Japan	3Q0110	**Filler:** silanated barium glass and pre-polymerized organic filler **Monomer:** bis-GMA and hydro-phobic aromatic dimethacrylate **Initiator:** dl-camphorquinone **Filler loading:** 78 wt%, 40 vol%	- Place the material into the cavity, light-cured for 20 seconds.
Clearfil™ SE bond X	Two-step self-etch adhesive system	Kuraray Noritake Dental Inc.; Japan	000059	**Primer:** MDP, HEMA, water, hydrophilic dimethacrylate, camphorquinone and N,N-diethanol p-toluidine **Adhesive:** MDP, HEMA, bis-GMA, hydrophobic dimethacrylate, camphorquinone, N,N-diethanol p-toluidine and silanated colloidal silica	- Agitate the primer to the cavity wall for 20 seconds and air-blow. - Apply adhesive and air-blow. - Light-cured for 10 seconds.
Adper™ Scotchbond™ multi-purpose	Three-step etch and rinse adhesive system	3M ESPE; USA	NA63739	**Etchant:** 37% phosphoric acid **Primer:** HEMA, polyalkenoic acid polymer and water **Adhesive:** bis-GMA, HEMA, tertiary amines and photoinitiator	-Apply phosphoric etchant for 30 seconds, rinse thoroughly with water then gently air dry. - Apply primer and air-blow. -Apply adhesive and air-blow. -Light-cured for 10 seconds.

Bis-GMA = Bisphenol A glycidyldimethacrylate, MDP = Methacryloyloxydecyl dihydrogen phosphate, HEMA = Hydroxyethylmethacrylate

cylindrical cavity with a diameter and depth of 2 mm was prepared. The prepared specimens were then randomly divided into 6 groups of 6 teeth each conforming to the restorative materials and adhesive systems used, Group 1; Glass ionomer (GI), Group 2; Ion-releasing resin composite (CN), Group 3; Ion-releasing resin composite along with a two-step self-etch adhesive system (CN+CSE), Group 4; Ion-releasing resin composite along with a three-step etch and rinse adhesive system (CN+SBMP), Group 5; Conventional resin composite along with a two-step self-etch adhesive system (RC+CSE) and Group 6; Conventional resin composite along with a three-step etch and rinse adhesive system (RC+SBMP). The restorative materials and the adhesives were employed according to each product instruction as mentioned in Table 1. The adhesive was applied to the cavity walls and light-cured with a light-curing machine (Bluephase® LED curing light, Ivoclar, Liechtenstein) with a light intensity of 1200 mW/cm^2 for 10 seconds. Subsequently, the material was placed into the cavity and light-cured with the same light source for 20 seconds, except for the GI group. Only the restoration surface of GI group was coated with an adhesive of the two-step self-etch adhesive system before being stored in de-ionized water.

After being stored in deionized water at 37°C for 24 hours, the outer surface of all restored specimens was serially polished with silicon carbine papers of 600, 800, 1000 and 1500 grit to eliminate the excess restorative materials and to define the boundary of prepared restoration, and then cleaned with an ultrasonic cleanser (Bio-Sonic® UC125: Whaledent Inc., USA) for 10 minutes. Afterwards, all specimen surfaces were covered with nail varnish leaving out half of the filling and its adjacent enamel for 1 mm beyond the margin in order to expose to the artificial caries induction, as shown in Figure 2.

Artificial caries induction by pH-cycling

All specimens were subjected to an artificial caries induction by pH-cycling process for 14 days; each specimen was submerged in an 8 ml of demineralizing solution (2.2 mM of $CaCl_2$, 2.2 mM of KH_2PO_4, 0.05 M of acetic acid, pH of 4.4) for 6 hours and in an 8 ml of remineralizing solution (1.5 mM $CaCl_2$, 0.9 mM KH_2PO_4, 0.15 M KCl, 20 mM cacodylate buffer, pH of 7.0) for 18 hours.[14] After 14 days of artificial caries induction, all specimens were perpendicularly sectioned through the buccal enamel

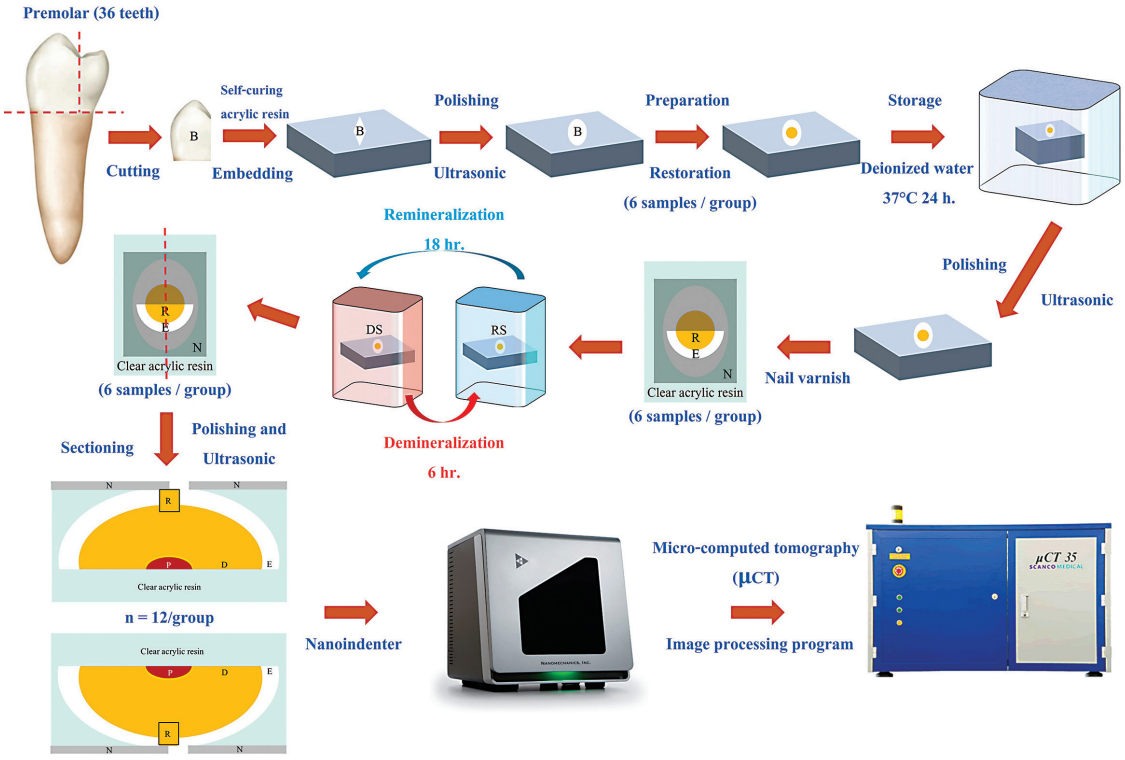

Figure 1: The procedures of specimen preparation and measurements. B: Buccal, R: Restoration, E: Enamel, N: Nail varnish, RS: Remineralization solution, DS: Demineralization solution, D: Dentin, P: Pulp

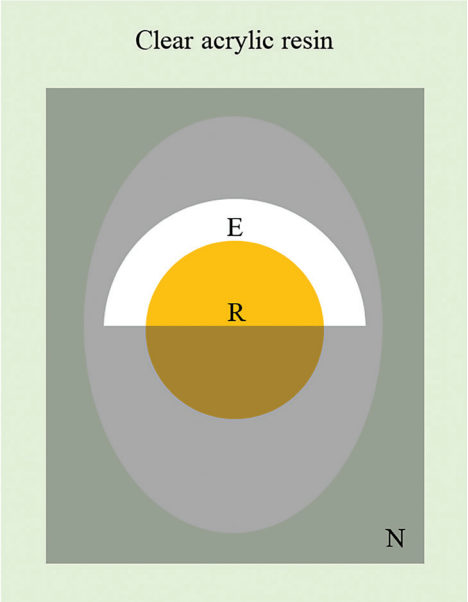

Figure 2: The enamel surface covered with nail varnish. R: Restoration, E: Enamel, N: Nail varnish

surface in an occluso-cervical direction to obtain two cross-sectional specimens (n=12). The sectioned surfaces were then serially polished with silicon carbine papers of 1000, 1500, 2000, 2500, 3000, 4000 and 5000 grit and cleaned in an ultrasonic cleanser for 10 minutes.

Nanohardness measurement

The cross-sectional specimen together with the indentation mapping are shown in Figure 3. The cross-sectional enamel indentations of both coated and uncoated nail varnish side were measured using a Berkovich nanoindenter with a maximam force of 10 mN at 1 mN/s loading rate by means of a nanoindentation machine (iMicro Indentation System, Nanomechanics, Inc., USA). Five indentations were performed on the nail varnish coated side (control group), the first indentation was located 10 μm from the restoration-enamel interface and the tooth surface. The second, third, fourth and fifth indentations also located at depth of 10 μm from the tooth surface but were 110, 210, 310 and 410 μm far from the restoration-enamel interface, respectively. The nanohardness values of the five indentations were averaged and recorded as a nanohardness value of each depth for each specimen. The uncoated nail varnish side was performed with twenty indentations. The first five indentations were located at the depth of 10 μm and designed according to the control group. The other fifteen indentation were located at the depths of 60, 110 and 160 μm from the tooth surface. Each depth was performed with five indentations in the same way as previously mentioned. For the specimens that the enamel surface was dissolved, the level of enamel surface was set up using the imaginary line between the restorative material surface and the outer enamel surface, which was coated with nail vanish.

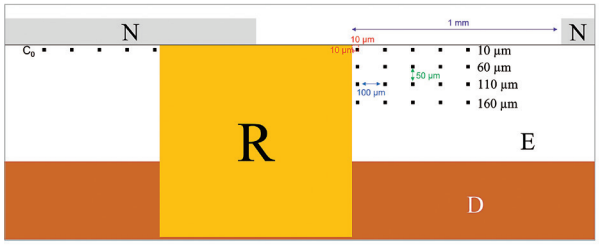

Figure 3: The cross-sectional specimen together with the indentation mapping. R: Restoration, E: Enamel, D: Dentin, N: Nail varnish

Mineral loss and lesion depth measurement

The cross-sectional specimen together with the locations of the mineral loss and lesion depth measurements are shown in Figure 4. Both values were performed at a condition of 70 kV voltage and 114 μA current, and 5 μm voxel dimensions by a micro computed tomography (microCT35; SCANCO Medical AG, Switzerland) and an image processing program (Rasband, W.S., ImageJ, U. S. National Institutes of Health, USA). The radiolucency and radiopacity of the micro-CT images were calibrated with a standard mineral content by using an image processing program to obtain the mineral profile of each specimen. Each mineral profile was processed for the mineral loss (ΔZ) and the lesion depth (LD) data. The mineral loss is the integrated difference of mineral volume between the sample and that of sound tooth structure. In addition, the lesion depth is the distance where the mineral content reaches 95% compared to that of sound enamel.[15]

Both measurements were tested at four distances from the restoration-enamel interface. Moreover, each distance was measured across a depth of 500 μm from the tooth surface. The first distance was measured at 10 μm from the restoration-enamel interface. The second, third and fourth distances were measured at 260, 510 and 760 μm from the restoration-enamel interface, respectively.

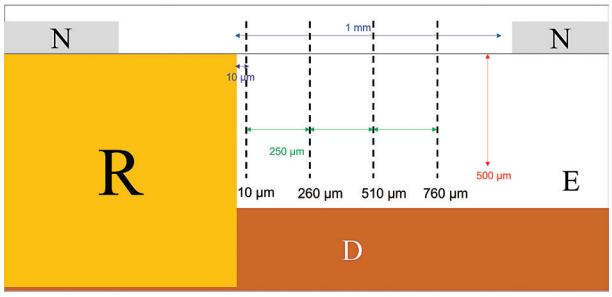

Figure 4: The cross-sectional specimen together with the locations for the mineral loss and lesion depth measurements. R: Restoration, E: Enamel, D: Dentin, N: Nail varnish

Statistical analysis

The statistical analysis was performed with IBM SPSS Statistics Version 25 (IBM Corporation, Armonk, NY, USA). All statistical analysis were tested at a 95% level of confidence. All collected data sets were subjected to normality and homogeneity tests to determine if the data set was distributed according to the normal distribution, and to prove the homogeneity of variances. The nanohardness values were compared within the same group using the Wilcoxon-signed rank test. The nanohardness values were compared among the 6 groups using the Kruskal-Wallis test. The mineral loss and lesion depth values were compared within the same group using the repeated measures ANOVA and Dunnett T3. Additionally, the mineral loss and lesion depth values were compared among the 6 groups using the One-way ANOVA and Dunnett T3.

Results

Enamel nanohardness values at different depths for each group are presented in Table 2. Due to the artificial caries induction, the RC groups exhibited the surface enamel dissolution at the depths of 10 and 60 μm. Therefore, the enamel nanohardness of these depths could not be measured. Whereas the GI, CN, CN+CSE and CN+SBMP group exhibited partial dissolution at the depths of 10 μm from the surface enamel resulting in the diversity of the population of each subgroup, which is presented in Figure 5. Within the same material group, the contiguous enamel of the GI, CN, CN+CSE and CN+SBMP group showed significantly lower nanohardness value at the depth of 10 and 60 μm compared to those of the control side (C_{10}) ($p<0.05$). However, there were no significant difference in the nanohardness values at the depth of 110 and 160 μm compared to those of the control side ($p>0.05$). On the other hand, the nanohardness values of contiguous enamel of the RC+CSE and RC+SBMP group were decreased significantly at the depth of 110 μm ($p<0.05$).

When comparing the nanohardness values of the contiguous enamel at the same depth, there were no significant differences between the GI, CN, CN+CSE and CN+SBM group at almost all the depths of measurements ($p>0.05$). However, at the depth of 10 μm from the tooth surface the CN+CSE and CN+SBM group exhibited significantly lower nanohardness values compared to those of the GI and CN group ($p<0.05$). The RC groups

Table 2: Means and standard deviations of the enamel nanohardness at different depths for each group after the 14 days of artificial caries induction.

Row	Group					
	GI (GPa)	CN (GPa)	CN+CSE (GPa)	CN+SBMP (GPa)	RC+CSE (GPa)	RC+SBMP (GPa)
C10	3.82 ± 0.56^{aA} (n=12)	3.76 ± 0.54^{aA} (n=12)	3.72 ± 0.50^{aA} (n=12)	3.73 ± 0.45^{aA} (n=12)	3.91 ± 0.63^{aA} (n=12)	3.68 ± 0.60^{aA} (n=12)
10 μm	1.93 ± 0.82^{cA} (n=12)	1.52 ± 0.52^{cAB} (n=11)	1.22 ± 0.71^{cB} (n=10)	0.97 ± 0.47^{cB} (n=9)	N/A	N/A
60 μm	3.22 ± 0.84^{bA} (n=12)	3.17 ± 0.86^{bA} (n=12)	3.15 ± 0.81^{bA} (n=12)	3.22 ± 0.64^{bA} (n=12)	N/A	N/A
110 μm	3.81 ± 0.73^{aA} (n=12)	3.76 ± 0.52^{aA} (n=12)	3.67 ± 0.60^{aAB} (n=12)	3.66 ± 0.88^{aAB} (n=12)	2.98 ± 0.89^{bBC} (n=12)	2.22 ± 0.93^{bC} (n=12)
160 μm	3.67 ± 0.84^{aA} (n=12)	3.72 ± 0.64^{aA} (n=12)	3.71 ± 0.76^{aA} (n=12)	3.61 ± 0.59^{aA} (n=12)	3.84 ± 0.44^{aA} (n=12)	3.46 ± 0.66^{aA} (n=12)

Different superscript lowercase letters indicate statistically significant differences within the same column ($p<0.05$). Different superscript uppercase letters indicate statistically significant differences within the same row ($p<0.05$).

Table 3: Means and standard deviations of the mineral loss at different distances for each group after the 14 days of artificial caries induction.

Group	Column			
	1 (10 μm) (mgHAP/m^2)	**2 (260 μm)** (mgHAP/m^2)	**3 (510 μm)** (mgHAP/m^2)	**4 (760 μm)** (mgHAP/m^2)
GI	2157.60±434.46^{aA}	16746.61±4534.05^{bA}	24662.67±4256.13^{cA}	40574.74±12043.82^{dA}
CN	3103.01±742.73^{aAB}	31239.09±7849.53^{bB}	44918.33±2943.97^{cB}	46001.51±10069.08^{cA}
CN+CSE	4266.36±744.30^{aBC}	29113.04±6743.79^{bB}	41767.76±8080.23^{cB}	45055.42±7371.10^{cA}
CN+SBMP	5424.43±1208.41^{aC}	30862.01±7932.30^{bB}	47918.36±10001.06^{cB}	54916.60±10677.90^{cA}
RC+CSE	40769.21±8193.38^{aD}	79062.99±11761.57^{bC}	75027.58±10940.39^{bC}	78962.31±10940.39^{bB}
RC+SBMP	48315.46±2941.34^{aD}	96352.93±16827.34^{bC}	90859.19±12402.10^{bC}	88125.82±12299.67^{bB}

Different superscript lowercase letters indicate statistically significant differences within the same row (p<0.05). Different superscript uppercase letters indicate statistically significant differences within the same column (p<0.05).

Table 4: Means and standard deviations of the lesion depth at different distances for each group after the 14 days of artificial caries induction.

Group	Column			
	1 (10 μm) (μm)	**2 (260 μm)** (μm)	**3 (510 μm)** (μm)	**4 (760 μm)** (μm)
GI	17.19±8.36^{aA}	70.60±18.92^{bA}	93.62±25.93^{cA}	135.19±39.24^{dA}
CN	24.08±9.99^{aAB}	115.81±28.94^{bB}	148.61±30.33^{cB}	157.94±39.21^{cAB}
CN+CSE	30.68±5.81^{aB}	102.53±10.19^{bB}	137.46±21.36^{cB}	172.01±33.14^{cAB}
CN+SBMP	33.82±3.94^{aB}	116.91±26.38^{bB}	152.69±13.79^{cB}	162.01±14.81^{cAB}
RC+CSE	118.00±13.69^{aC}	170.80±32.67^{bC}	192.78±12.81^{bC}	194.90±23.37^{bB}
RC+SBMP	138.64±17.38^{aC}	203.26±35.61^{bC}	212.52±17.33^{bC}	206.76±35.32^{bB}

Different superscript lowercase letters indicate statistically significant differences within the same row (p<0.05). Different superscript uppercase letters indicate statistically significant differences within the same column (p<0.05).

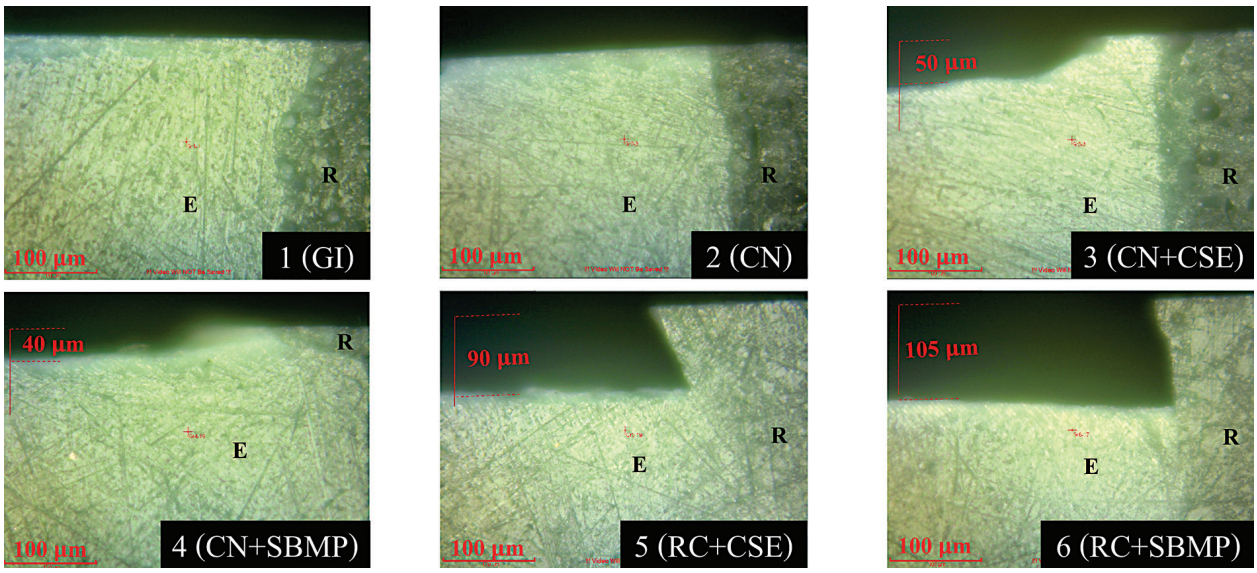

Figure 5: Microscopic images from the nanoindentation machine of the enamel adjacent to each restoration group after submerged for 14 days with the artificial caries induction (800X magnification). E: Enamel, R: Restoration

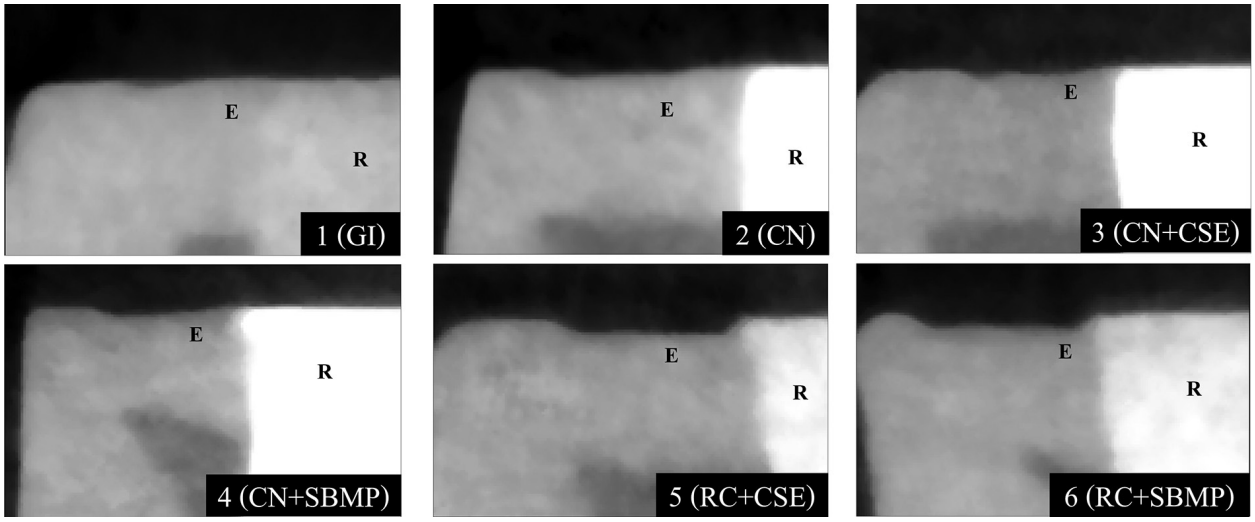

Figure 6: X-ray images from the micro-CT machine of the enamel adjacent to each restoration group after submerged for 14 days with the artificial caries induction. E: Enamel, R: Restoration

not only demonstrated the dissolution of the contiguous enamel, but also showed significantly lower nanohadness values at the depth of 110 μm compared to all the other groups. However, there were no significant difference in the nanohardness values of all experimental groups at the depth of 160 μm (p>0.05).

The mineral loss and lesion depth values of the contiguous enamel at different distances for each group are presented in Table 3 and 4, respectively. In addition, the x-ray images from the micro-CT machine of each group are presented in Figure 6. When the mineral loss and lesion depth values were compared within the same group, only the GI group showed significant differences among the different distances from the restoration-enamel interface (p<0.05). When comparing the mineral loss and lesion depth values among the groups at the distance of 10 μm, the GI group showed significant differences among the other groups except for the CN group. However, only the mineral loss values between the CN and CN+SBMP group showed a significant difference at the depth of 10 μm (p<0.05). The mineral loss and lesion depth values at the depth of 260 and 510 μm showed significant differences among the different material groups of GI, CN and RC, but no significant differences were observed within the same material group.

Discussion

The pH in the oral cavity is dynamic, which results in an episodic change of demineralization and remineralization. The demineralization of tooth enamel commenced when the pH decreases below 4.5 and 5.5 for fluorapatite and hydroxyapatite, respectively.[16] Ion-releasing restorative materials that mainly release fluoride ions of which inhibits demineralization, enhance remineralization and also has bactericidal effects. The role of these properties are to prevent secondary caries from developing.[6] Moreover, the alkasite material can release other ions; calcium ions that acts as a reservoir, which maintains the level of ions and enhances remineralization.[17] Hydroxyl ions with a buffer capacity that neutralizes the acidic conditions.[18] As a result of these ions, the caries inhibition effect of the surrounding tooth structure could be achieved. Caries inhibition effects can be detected into 2 categories; the first is the caries inhibition zone, which is a tooth structure formed by fluoride ions from fluoride-releasing restorations. This zone can protect against acidic conditions more effectively than that of normal tooth structures.[19] The second is the acid-base resistance zone, which is a tooth layer formed beyond the hybrid layer by acidic functional monomers in the self-etch adhesive systems. This zone increases the resistance of the tooth structure against acidic and basic conditions greater than that of sound tooth structure.[20,21] Previous studies reported that 10-MDP, as an acidic functional monomer, formed the most durable layer of the acid-base resistance zone among the other functional monomers.[22,23]

In this study, the mechanical property of the enamel adjacent to the restoration was tested by a cross-sectional

nanoindentation method. Furthermore, the quantitative measurements of the mineral loss and lesion depth were tested using the Micro-CT together with the image processing program. These methods indicate the material's ability to inhibit enamel demineralization during the artificial caries induction process.[11,15,24,25]

The enamel nanohardness values in this study exhibited remarkable differences among the ion-releasing material groups (GI, CN, CN+CSE and CN+SBMP) and the non ion-releasing material groups (RC+CSE and RC+SBMP) at the depth of 10 and 60 μm. At these depths, the groups of GI, CN, CN+CSE and CN+SBMP exhibited only partial enamel dissolution, therefore the nanohardness values could be measured. Whereas the nanohardness of the RC+CSE and RC+SBMP group could not be measured due to complete enamel dissolution at these depths. The nanohardness values that differed among the material groups correspond with previous studies, which reported that the artifical caries induction resulted in a demineralization of the enamel adjacent to the glass ionomer material and a reduction of 7 percent in microhardness compared with that of sound enamel. While the non fluoride-releasing resin composite caused a 44 percent reduction of enamel microhardness.[26] In addition, these results also correspond with the study of Serra MC and Cury JA. After the artificial caries induction, the conventional resin composite group exhibited a lower microhardness of the contiguous enamel than that of glass ionomer cement and sound enamel at the depth of 30 μm from the enamel surface. While the nanohardness values at the depth of 130 and 230 μm exhibited no significant differences among the groups.[10] In this study, the enamel at greater depths exhibited greater nanohardness values. At the depth of 160 μm, the enamel nanohadness had no significant differences among the different groups and with the control group. This could have been caused by the artificial caries induction process, which had a lower effect to the enamel at the greater depths.

When comparing the mineral loss and lesion depth values within the same group, the GI was the only group that exhibited significant differences among the value of each distance. These results could be related to the different materials, which release different quantities of ions especially fluoride ions. The manufacturer reported that at the different conditions of pH 4.0 and 6.8, the glass ionomer (Fuji IX GP Fast®) released a greater amount of fluoride ions than Cention N. However, Cention N can release calcium and hydroxyl ions that are undetectable with the glass ionomer material.[8] These findings corresponded with other studies, which reported that the enamel in close vicinity to the restorations exhibited the highest degree of protection against demineralization. Moreover, the mineral loss and lesion depth increased when the enamel was further away from restoration. These values were inversely related with the amount of fluoride ions released from the restoration.[27,28] In this study, at the distance of 10 μm from the restoration-enamel interface, the mineral loss and lesion depth of the GI group showed significantly lower values among the other groups, except for the CN group. However, further away from the restoration at the distance of 260 and 510 μm, the GI groups had the lowest values and were significantly lower among the other groups. This corresponds with the study of Tantbirojn D *et al.,* which reported that the enamel adjacent and up to 7 mm from the glass ionomer materials exhibited significant reductions of mineral loss values.[29] For the fluoride-releasing resin composite, the mineral loss only reduced at the enamel in close vicinity to the material but no effect was observed at 3 to 4 mm from the restoration.[30] In addition, the enamel adjacent to the conventional glass ionomer material exhibited a lesion depth shallower compared to the non-fluoridated materials by 58-80%, while fluoride-releasing resin composites exhibited a lesion depth shallower by 9-40%.[28]

At the distance of 10 μm from the restoration-enamel interface, there were no significant differences between the mineral loss value of the CN+CSE group and the CN+SBMP group. However, the CN group exhibited a significantly lower mineral loss value than that of CN+SBMP group. Furthermore, at the depth of 10 μm from the enamel surface, the contiguous enamel of the GI and the CN group demonstrated no significant difference in the nanoharness values. The GI group noticeably exhibited a significantly higher enamel nanohardness value among that of CN+CSE and CN+SBM group. These results could be related to the adhesive layer, which could hamper the effectiveness of released ions from the material to the adjacent tooth structures. This finding corresponds with the study of Itota T *et al.,* which reported that the cavity wall applied with adhesive interrupted the fluoride release from the fluoride-releasing resin composites.[31] At the distances of 10, 260 and 510 μm from the resto-

ration-enamel interface, the CN+CSE and CN+SBMP groups exhibited significantly lower mineral loss and lesion depth values than that of RC+CSE and RC+SBMP group. This finding also corresponds with a previous study, where the authors stated that caries inhibition effect was mainly controlled by fluoride ions released from the material's surface onto the adjacent tooth surface, while the inhibition was least influenced by the small amounts of fluoride ions penetrated through the adhesive layer.[31] Consequently, the cavity wall without the adhesive layer could influence the uptake of fluoride ions on both the outer tooth surface and the cavity wall. However, the ion-releasing material accompanying the application of adhesive (CN+CSE and CN+SBMP), demonstrated greater caries inhibition effect to the adjacent enamel than that of non ion-releasing material (RC+CSE and RC+SBMP).

The carious process induces the occurring of white spot lesion. This lesion is developed at the enamel's subsurface layer by porous formations of which affect the refractive index and roughness.[32,33] Moreover, the enamel with white spot lesion demonstrated lower hardness and mineral density values compare to those of sound enamel.[34,35] In the present study, the caries inhibition effect was investigated after 14 days of artificial caries induction using 3 parameters, the nanohardness, the mineral loss and the lesion depth values of each experimental group. Other studies reported that the white spot lesion exhibited a reduction of nanohardness values by 42.5-91% compared to its sound enamel.[34,35] In this study, the four groups of GI, CN, CN+CSE and CN+SBMP exhibited a nanohardness reduction. These values were reduced at a range of 49.5-75, 16-17 and 0-2% for the depths of 10, 60 and 110 μm, respectively. On the other hand, the two groups of RC+CSE and RC+SBMP exhibited surface enamel dissolution at the depths of 10 and 60 μm, as a result, the nanohardness values could not be measured. However, at the depth of 110 μm, these two groups exhibited a nanohardness reduction of 25-40%. These results suggested that the 14 days of artificial caries induction process potentially induces the white spot lesion at the depth of approximately 60-110 μm and indicated that the four ion-releasing material groups could identify the caries inhibition effect at the depths of 60 μm, and the two groups of non ion-releasing materials exhibited no caries inhibition property.

The mineral loss of the white spot lesion from other studies exhibited a reduction of 17-50% compared to its sound counterparts.[36,37] In this study, at the distances of 10, 260 and 510 μm from the restoration-enamel interface, the GI group exhibited lower mineral loss values than that of the white spot lesion, while the CN, CN+CSE and CN+SBMP group only exhibited lower values at the distances of 10 μm. On the other hand, the RC+CSE and RC+SBMP exhibited greater values than that of white spot lesions at all distances. The lesion depths of the white spot lesion from other studies exhibited between 100-500 μm.[36,37] The relations of the lesion depth were the same as the mineral loss that were previously mentioned. Therefore, in the present study, the caries inhibition effect of the enamel adjacent to the restoration differs among the different materials of which were used to restore the cavity.

Conclusions

The null hypothesis of this study was rejected. The results of this *in vitro* study indicated that the glass ionomer and ion-releasing resin composite materials demonstrated significantly greater caries inhibition effect on the adjacent enamel compared with that of conventional resin composite. The ion-releasing resin composite without adhesive application exhibited greater caries inhibition of adjacent enamel compared with this material used with adhesive. In addition, the different adhesive systems had no significant effect on caries inhibition property of the ion-releasing resin composite.

Acknowledgments

The authors would like to acknowledge Dr. Thanapat Sastraruji at Dental research center, Faculty of Dentistry, Chiang Mai University for his assistance with the nanoindentation and the statistical analysis.

Conflict of interest

The authors declare no conflict of interest.

References

1. Fisher J, Varenne B, Narvaez D, Vickers C. The minamata convention and the phase down of dental amalgam. Bull World Health Organ. 2018;96(6):436-8.
2. Arola D, Galles LA, Sarubin MF. A comparison of the mechanical behaviour of posterior teeth with amalgam and composite MOD restorations. J Dent. 2001;29(1):63-73.

3. Carvalho RM, Pereira JC, Yoshiyama M, Pashley DH. A review of polymerization contraction: the influence of stress development versus stress relief. Oper Dent. 1996;21(1): 17-24.
4. Schneider LF, Moraes RR. Polymerization shrinkage stress. Dental composite materials for direct restorations. Vol I: Springer, Cham; 2018. 219-33.
5. Mjör IA, Qvist V. Marginal failures of amalgam and composite restorations. J Dent. 1997;25(1):25-30.
6. Wiegand A, Buchalla W, Attina T. Review on fluoride-releasing restorative materials-fluoride release and uptake characteristics, antibacterial activity and influence on caries formation. Dent Mater. 2007;23(3):343-62.
7. van Dijken JW, Kalfas S, Litra V, Oliveby A. Fluoride and mutans streptococci levels in plaque on aged restorations of resin-modified glass lonomer cement, compomer and resin composite. Caries Res. 1997;31(5):379-83.
8. Todd JC. Scientific Documentation: Cention N; Ivoclar-Press: Schaan, Liechtenstein. 2016:1-58.
9. Tiskaya M, Al-Eesa NA, Wong FSL, Hill RG. Characterization of the bioactivity of two commercial composites. Dent Mater. 2019;35(12):1757-68.
10. Serra MC, Cury JA. The *in vitro* effect of glass-ionomer cement restoration on enamel subjected to a demineralization and remineralization model. Quintessence Int. 1992;23(2):143-7.
11. Zou W, Hunter N, Swain MV. Application of polychromatic microCT for mineral density determination. J Dent Res. 2011;90(1):18-30.
12. Habelitz S, Marshall SJ, Marshall Jr GW, Balooch M. Mechanical properties of human dental enamel on the nanometre scale. Arch Oral Biol. 2001;46(2):173-83.
13. Ge J, Cui FZ, Wang XM, Feng HL. Property variations in the prism and the organic sheath within enamel by nanoindentation. Biomater. 2005;26(16):3333-9.
14. Ten Cate JM, Duijsters PP. Alternating demineralization and remineralization of artificial enamel lesions. Caries Res. 1982;16(3):201-10.
15. Arends J, Ten Bosch JJ. Demineralization and remineralization evaluation techniques. J Dent Res. 1992;71(3):924-8.
16. Larsen MJ, Pearce EIF. Saturation of human saliva with respect to calcium salts. Arch Oral Biol. 2003;48(4):317-22.
17. Frankenberger R, Garcia-Godoy F, Lohbauer U, Petschelt A, Krämer N. Evaluation of resin composite materials. Part I: *in vitro* investigations. Am J Dent. 2005;18(1):23-7.
18. Persson A, Lingstrom P, van Dijken JW. Effect of a hydroxyl ion-releasing composite resin on plaque acidogenicity. Caries Res. 2005;39(3):201-6.
19. Itota T, Nakabo S, Iwai Y, Konishi N, Nagamine M, Torii Y, *et al*. Effect of adhesives on the inhibition of secondary caries around compomer restorations. Oper Dent. 2001;26(5):445-50.
20. Tsuchiya S, Nikaido T, Sonoda H, Foxton RM, Tagami J. Ultrastructure of the dentin-adhesive interface after acidbase challenge. J Adhes Dent. 2004;6(3):183-90.
21. Takagiki T, Nikaido T, Tsuchiya S, Ikeda M, Foxton RM, Tagami J. Effect of hybridization on bond strength and adhesive interface after acid-base challenge in 4-META/MMA-TBB resin. Dent Mater J. 2009;28(2):185-93.
22. Nurrohman H, Nikaido T, Takagaki T, Sadr A, Ichinose S, Tagami J. Apatite crystal protection against acid-attack beneath resin–dentin interface with four adhesives: TEM and crystallography evidence. Dent Mater. 2012;28(7): 89-98.
23. Li N, Nikaido T, Takagaki T, Sadr A, Makishi P, Chen J, *et al.* The role of functional monomers in bonding to enamel: acid-base resistant zone and bonding performance. J Dent. 2010;38(9):722-30.
24. Willems G, Celis J, Lambrechts P, Braem M, Vanherle G. Hardness and young's modulus determined by nanoindentation technique of filler particles of dental restorative materials compared with human enamel. J Biomed Mater Res. 1993;27(6):747-55.
25. Angker L, Swain MV. Nanoindentation: application to dental hard tissue investigations. J Mater Res. 2006;21(8): 1893-905.
26. Kreulen CM, de Soet JJ. *In vivo* cariostatic effect of resin modified glass ionomer cement and amalgam on dentine. Caries Res. 1997;31(5):384-9.
27. Ferracane JL, Mitchem JC, Adey JD. Fluoride penetration into the hybrid layer from a dentin adhesive. Am J Dent. 1998;11(1):23-8.
28. Dionysopoulos D, Koliniotou-Koumpia E, Helvatzoglou-Antoniades M, Kotsanos N. *In vitro* inhibition of enamel demineralisation by fluoride-releasing restorative materials and dental adhesives. Oral Health Prev Dent. 2016;14(4):371-80.
29. Tantbirojn D, Douglas WH, Versluis A. Inhibitive effect of a resin-modified glass lonomer cement on remote enamel artificial caries. Caries Res. 1997;31(4):275-80.
30. Dijkman GE, de Vries J, Lodding A, Arends J. Long-term fluoride release of visible light-activated composites *in vitro*: a correlation with *in situ* demineralisation data. Caries Res. 1993;27(2):117-23.
31. Itota T, Nakabo S, Narukami T, Tashiro Y, Torii Y, McCabe JF, *et al.* Effect of two-step adhesive systems on inhibition of secondary caries around fluoride-releasing resin composite restorations in root dentine. J Dent. 2005;33(2):147-54.
32. Yun F, Swain MV, Chen H, Cairney J, Qu J, Sha G, *et al*. Nanoscale pathways for human tooth decay–central planar defect, organic-rich precipitate and high-angle grain boundary. Biomaterials. 2020;235:119748.doi: 10.1016/j.biomaterials.2019.

33. Guerra F, Mazur M, Nardi GM, Corridore D, Pasqualotto D, Rinado F, *et al.* Dental hypomineralized enamel resin infiltration. clinical indications and limits. Senses Sci. 2015;2(4):135-9.
34. Sadyrin E, Swain M, Mitrin B, Rzhepakovsky I, Nikolaev A, Irkha V, *et al.* Characterization of enamel and dentine about a white spot lesion: mechanical properties, mineral density, microstructure and molecular composition. Nanomaterials (Basel). 2020;10(9):1889. doi: 10.3390/nano10091889.
35. Huang TT, He LH, Darendeliler MA, Swain MV. Nanoindentation characterisation of natural carious white spot lesions. Caries Res. 2010;44(2):101-7.
36. Cochrane NJ, Anderson P, Davis GR, Adams GG, Stacey MA, Reynolds EC. An x-ray microtomographic study of natural white-spot enamel lesions. J Dent Res. 2012;91(2):185-91.
37. Huang TT, He LH, Darendeliler MA, Swain MV. Correlation of mineral density and elastic modulus of natural enamel white spot lesions using X-ray microtomography and nanoindentation. Acta Biomater. 2010;6(12):4553-9.